British Journal of Pharmacology

DOI:10.1111/j.1476-5381.2012.02083.x
www.brjpharmacol.org

RESEARCH PAPER

Allosteric nature of P2X receptor activation probed by photoaffinity labelling

Y Bhargava*, J Rettinger‡ and A Mourot†

Department of Biophysical Chemistry, Max-Planck-Institute of Biophysics, Frankfurt am Main, Germany

Correspondence
Yogesh Bhargava and Alexandre Mourot, Department of Biophysical Chemistry, Max-Planck-Institute of Biophysics, Max-von-Laue-Straße 3, 60438 Frankfurt am Main, Germany. E-mail: y.bhargava@wibr.ucl.ac.uk; almourot@gmail.com

*Present address: Wolfson Institute for Biomedical Research, University College London, Gower Street, London WC1E 6BT, UK.
†Present address: Université P. et M. Curie, CNRS UMR 7102, Neurobiologie des Processus Adaptatifs, Neurophysiologie and Behavior Team, 75005 Paris, France.
‡Present address: Multi Channel Systems MCS GmbH, Aspenhaustraße 21, 72770 Reutlingen, Germany.

Keywords
P2X receptors; allosteric activation; binding; gating; photolabelling; ion channel

Received
14 December 2011
Revised
29 May 2012
Accepted
10 June 2012

BACKGROUND AND PURPOSE

In P2X receptors, agonist binding at the interface between neighbouring subunits is efficiently transduced to ion channel gating. However, the relationship between binding and gating is difficult to study because agonists continuously bind and unbind. Here, we covalently incorporated agonists in the binding pocket of P2X receptors and examined how binding site occupancy affects the ability of the channel to gate.

EXPERIMENTAL APPROACH

We used a strategy for tethering agonists to their ATP-binding pocket, while simultaneously probing ion channel gating using electrophysiology. The agonist 2′,3′-O-(4-benzoylbenzoyl)-ATP (BzATP), a photoaffinity analogue of ATP, enabled us to trap rat homomeric P2X2 receptor and a P2X2/1 receptor chimera in different agonist-bound states. UV light was used to control the degree of covalent occupancy of the receptors.

KEY RESULTS

Irradiation of the P2X2/1 receptor chimera – BzATP complex resulted in a persistent current that lasted even after extensive washout, consistent with photochemical tethering of the agonist BzATP and trapping of the receptors in an open state. Partial labelling with BzATP primed subsequent agonist binding and modulated gating efficiency for both full and partial agonists.

CONCLUSIONS AND IMPLICATIONS

Our photolabelling strategy provides new molecular insights into the activation mechanism of the P2X receptor. We show here that priming with full agonist molecules leads to an increase in gating efficiency after subsequent agonist binding.

Abbreviations

αβ-MetATP, αβ -methylene ATP; BzATP, 2′,3′-O-(4-benzoylbenzoyl)-ATP; I_{max}, maximum current; I_p, persistent current; TEVC, two-electrode voltage-clamp; TNP-ATP, trinitrophenyl ATP

Introduction

P2X receptors are expressed widely, not only throughout the nervous system (central, peripheral and autonomic) but also in leucocytes, platelets and muscles, making them important drug targets (Khakh and North, 2006). P2X receptors are ATP-gated, non-selective cation channels that represent the third superfamily of ligand-gated ion channels apart from cys-loop receptors and ionotropic glutamate receptors (Valera *et al.*, 1994; Le Novere and Changeux, 1999). In mammals, seven P2X subunits have been identified. They self-assemble as homo- or heterotrimers to form functional receptors (for review, see North and Surprenant, 2000; North, 2002). Biochemical and structural studies revealed that P2X receptors have a trimeric architecture, with three ATP-binding sites located at the interface between neighbouring subunits (Aschrafi *et al.*, 2004; Barrera *et al.*, 2005; Marquez-Klaka *et al.*, 2007; Kawate *et al.*, 2009; Jiang *et al.*, 2011). Despite the progress being made, our understanding of the activation mechanism of P2X receptors is still limited.

In P2X receptors, binding of agonists allosterically triggers gating of the channel through cooperative interactions between the subunits (Ding and Sachs, 1999; Marquez-Klaka *et al.*, 2007; Li *et al.*, 2008; Evans, 2009). However, insights into the relationship between those two events, binding and gating, are difficult to gain, even at the single-channel level because ligands continuously bind to, and dissociate from, their sites (Karpen and Ruiz, 2002). One strategy for relating ligand binding to channel gating is to follow simultaneous binding using a fluorescent agonist and channel activation using electrophysiological recordings (Biskup *et al.*, 2007). Another strategy is to photochemically tether agonists to their binding pockets in order to prevent ligand dissociation (Brown *et al.*, 1993; Karpen and Brown, 1996; Ruiz and Karpen, 1997; Mourot *et al.*, 2006; Forman *et al.*, 2007; Zhong *et al.*, 2008; Agboh *et al.*, 2009). The incorporation level of photoaffinity labels can be precisely controlled because light is used as a trigger for the chemical reaction, enabling electrophysiological study of receptors in different agonist-bound states (Ruiz and Karpen, 1997).

In our study, we used 2′,3′-O-(4-benzoylbenzoyl)-ATP (BzATP) to photolabel rat homomeric P2X2 receptors and a P2X2/1 receptor chimera over-expressed in *Xenopus laevis* oocytes. BzATP and azido-ATP have been used previously to label P2X receptors (Erb *et al.*, 1990; Agboh *et al.*, 2009), but BzATP has some key advantages: it is stable under ambient light conditions, can be activated with wavelengths greater than 300 nm and maintains agonist profile on different P2X receptors (North and Surprenant, 2000; Agboh *et al.*, 2009). The P2X2/1 receptor chimera consists of the N-terminal and TM1 domains of the P2X2 receptor and the extracellular loop, TM2 and C-terminal domain of the P2X1 receptor (Werner *et al.*, 1996; Rettinger and Schmalzing, 2004). The P2X2/1 receptor chimera is a valid model for the P2X1 receptor and is particularly suited to our study because, like P2X1 receptors, it has a high potency to various ligands, and like P2X2 receptors, it does not desensitize (Rettinger and Schmalzing, 2004). We show here that BzATP can be efficiently incorporated into P2X receptors expressed in oocytes, producing persistent currents on the P2X2/1 receptor chimera while modulating efficacy and potency of other agonists.

Methods

Materials

ATP (disodium salt), αβ-methylene ATP (αβ-MetATP), benzophenone ATP (BzATP), trinitrophenyl ATP (TNP-ATP), collagenase, gentamicin, and HEPES were purchased from Sigma-Aldrich Chemie GmbH (Munich, Germany). *X. laevis* female frogs were obtained from Nasco International (Fort Atkinson, WI, USA). Other chemicals used were of highest purity grade available.

Frog maintenance

Ten to fifteen frogs were placed in a large tank of capacity ~ 200 L filled ~ 2/3 with fresh water free from chlorine. To avoid frog escape, each tank was covered with a grid in a wooden frame. For their well-being, each tank contained a few hiding sites (open ends cylinders of baked clay). Individual arrangements were made in each tank for continuous fresh water circulation. Temperature of water was maintained in the range of 16–19 °C. A 12/12h light/dark cycle was maintained by the use of one tungsten lamp. Beef heart pellets were used to feed the frogs twice a week. Tanks were regularly cleaned from any food debris in order to reduce microbial growth.

Surgical preparation

A small fish net was used to capture a healthy female from the tank and transfer it to a small box with a lid containing ~ 500ml of general anaesthetic consisting of 0.2 % solution (pH 7) of tricaine methanesulfonate (MS-222, Sigma) in tap water. Anaesthesia was applied by transferring the frog into the anesthesia solution for 10–15 min. The anaesthetized frog was then washed with distilled water to remove excess MS-222. The frog was placed on an ice box with dorsal side facing down. The ventral surface of the frog was covered with clean wet paper towels in order to protect the skin from drying. A small transectional cut was made with sterile scissors in one of the two lower quadrants of the abdomen by lifting the skin with sterile tweezers. Ovarian lobes were pulled out with the help of tweezers. A cut was made through the ovarian lobes in order to detach them from the frog's body. Ovarian lobes were then placed in calcium supplemented Oocyte Ringer solution until further use. The wall of the coelom (surgical cut in the abdomen) was closed using two to three simple interrupted sterile synthetic sutures, which included the skin, serosa and muscles. After the surgical procedure, the frog was placed in a small recovery tank for post surgical monitoring. Complete recovery usually occurred within 2–4 h. In the present study, oocytes from the 10 different frogs were used. All studies involving animals are reported in accordance with the ARRIVE guidelines (Kilkenny *et al.*, 2010; McGrath *et al.*, 2010).

cRNA synthesis and oocyte expression

Both P2X2 and P2X2/1 receptor chimera plasmid cDNA constructs (pNKS2-His6-rP2X2A and pNKS2-His6-rP2X2/1 respectively) were generously provided by Prof. Günther

Schmalzing, Department of Molecular Pharmacology, University Hospital Aachen, Germany. The construction of N-terminal hexahistidyl-tagged chimeric cDNA in the pNKS2 oocyte expression vector has been described previously (Nicke *et al.*, 1998; Rettinger and Schmalzing, 2004). Capped RNA was synthesized from linearized templates with SP6 RNA polymerase using the mMESSAGE mMACHINE kit (Ambion, Austin, TX, USA).

The *X. laevis* oocytes surgically removed from anaesthetized adult females were subjected to collagenase (2 mg·mL^{-1}) treatment (2–3 h) in oocyte Ringer's solution (ORI) (110 mM NaCl, 5 mM KCl, 2 mM $CaCl_2$, 1 mM $MgCl_2$, 5 mM HEPES, pH 7.5) and later washed several times with calcium-free ORI. Defolliculated oocytes of stage V or VI were manually selected and injected with 0.5 ng per cell cRNA for wild-type P2X2 and 5 ng per cell cRNA for the P2X2/1 receptor chimera. Injected cells were incubated in ORI containing 0.05 mg·mL^{-1} gentamicin at 18°C for 1–2 days before measurements.

Design of photolabelling setup

For simultaneous photolabelling and current measurement from the same set of receptors, we designed a custom-made oocyte recording chamber (Figure 1) (Mourot *et al.*, 2008). The recording chamber consisted of two compartments connected by a 0.6 mm diameter hole on which the oocyte was placed with the animal pole down. The upper compartment was continuously superfused with recording solution (MgORI: 90 mM NaCl, 1 mM KCl, 2 mM $MgCl_2$, 5 mM HEPES, pH 7.5) and provided access for the microelectrodes. Ligands were applied via a manifold to the lower compartment, which was sealed by a thin glass coverslip. A quartz optic fibre (diameter 1 mm) transmitted high-intensity UV light (λ_{max} = 366 nm with energy = 10 mJ at 410 nm) from a 100 W HBO lamp to the bottom of the chamber. The portion of the oocyte exposed to agonist was also entirely within the area of the fibre optic tip. This enabled efficient ligand perfusion and photolabelling of the same population of receptors. UV light was applied for photolabelling only when the maximum amplitude of current was reached during each BzATP application. The time of UV-light irradiation was manually controlled using a shutter placed between the HBO lamp and the quartz optic fibre.

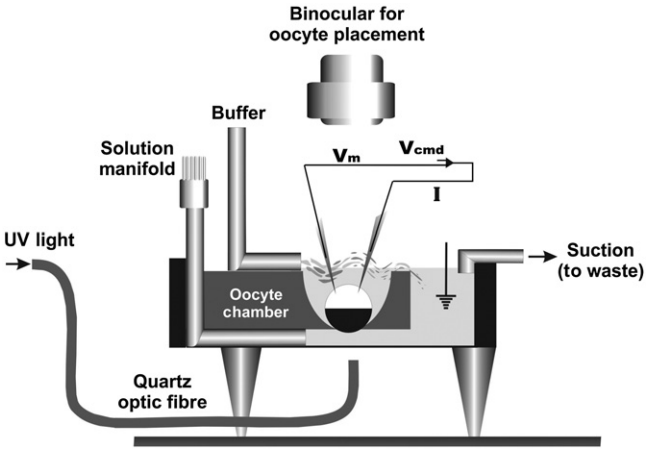

Figure 1

Design of the oocyte photolabelling chamber. Custom-made recording chamber for concurrent photolabelling and electrophysiological measurements from the same population of P2X receptors overexpressed in *Xenopus laevis* oocytes. UV light was transmitted from an HBO lamp to the chamber by quartz optic fibre. Ligands were applied using a solution manifold.

Functional measurement of receptors

Current responses to various ligands were measured using the two-electrode voltage-clamp (TEVC) method 1–2 days after cRNA injection into *X. laevis* oocytes. As P2X receptors are permeable to calcium ions, calcium salts were omitted from the recording solutions to avoid the activation of calcium-activated chloride channels. All measurements were performed in MgORI. TEVC was performed either in an ~50 µL recording chamber perfused at a flow rate of ~10 mL·min^{-1} (Rettinger and Schmalzing, 2003) or by using the custom-made oocyte recording chamber described earlier. Solutions were switched by software-controlled magnetic valves. Two intracellular glass microelectrodes with a resistance of <1 MΩ were used to clamp the oocytes at −60 mV. Currents were recorded with the TEC-03X amplifier (NPI Electronics, Lambrecht, Germany), low pass filtered at 100 Hz and sampled at >200 Hz (INT-20X AD/DA converter) using CELL-WORKS software (NPI Electronics). All measurements were performed at room temperature (20–22°C). All data are presented as mean ± SEM for the indicated number of experiments (*n*). EC_{50} values were calculated from dose–response curves obtained from a non-linear fit of the Hill equation using ORIGIN software (OriginLab, Northampton, MA, USA). All graphs were plotted in ORIGIN v7.5 or v8 software. Significance was calculated by *t*-test and *P*-values are reported where significant.

Results

Efficacy and potency of different ligands on P2X2 and P2X2/1 chimera receptors

We found BzATP to be a partial agonist for P2X2 receptors, in agreement with previous reports (North and Surprenant, 2000). A saturating concentration of BzATP (300 µM) elicited ~20% of the current responses elicited by a saturating concentration of ATP (300 µM) (Figure 2A,B and Table 1).

In contrast, BzATP and αβ-MetATP are full agonists for the P2X2/1 receptor chimera when compared with ATP. Current traces elicited by saturating concentrations of ATP, BzATP and αβ-MetATP (1 µM each) generated currents of similar amplitude (Figure 2C,D). Surprisingly, TNP-ATP, a potent antagonist of P2X1 receptors with an IC_{50} of 1 nM (North and Surprenant, 2000; Virginio *et al.*, 1998), elicited receptor currents (<2% at saturating concentration), suggesting that it is also an agonist with very low efficiency for the P2X2/1 receptor chimera (Figure 2E). Rapid desensitization of P2X1 may mask the very weak agonist properties of TNP-ATP. On the P2X2/1 receptor chimera, ATP has the highest potency, followed by BzATP and αβ-MetATP (Figure 2F and Table 1).

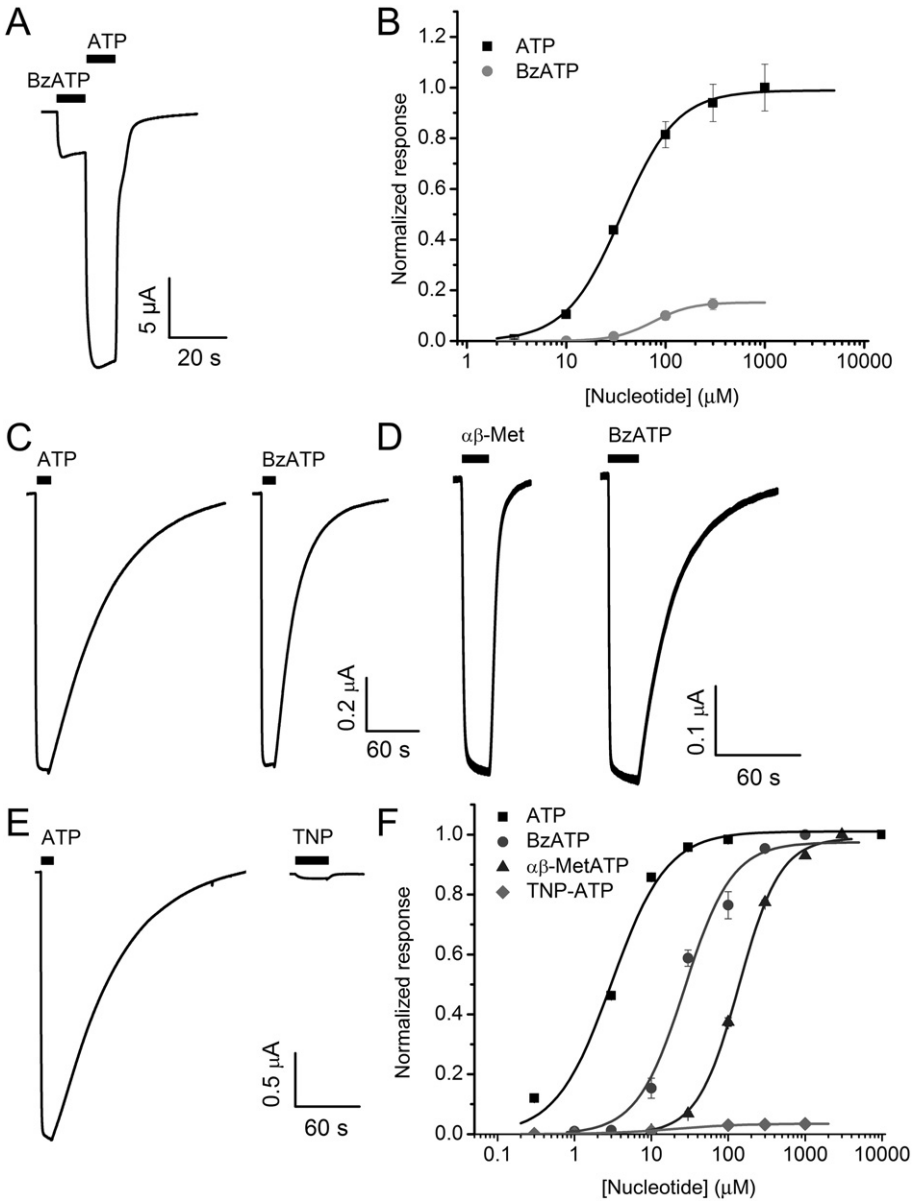

Figure 2

Efficacy and potency of different ligands on P2X2 and P2X2/1 receptor chimera. (A) Representative current trace of saturating concentration of BzATP (300 μM) and ATP (300 μM) on the same oocyte expressing wild-type P2X2 receptors. (B) Dose–response curves for ATP and BzATP on P2X2 receptors. Data are presented as mean ± SEM of 5 cells for each ligand concentration. Representative current traces for the P2X2/1 receptor chimera: (C) 1 μM ATP and 1 μM BzATP; (D) 1 μM αβ-MetATP and 1 μM BzATP; and (E) 1 μM ATP and 100 nM TNP-ATP were applied on the same oocyte. (F) Dose–response curves for various ligands on the P2X2/1 receptor chimera. All responses were normalized to the response generated by the saturating concentration of the respective full agonists. Data are represented as mean ± SEM for 4–34 cells for each concentration.

Occupancy with a partial agonist decreases the full agonist response at the P2X2 receptor

We asked whether BzATP could be photo-incorporated into P2X2 receptors expressed in oocytes. We perfused BzATP (30 μM) on a portion of the voltage-clamped oocyte expressing P2X2 and illuminated the same part of the cell with UV light (Figure 1). Because BzATP currents were very small, covalent incorporation was assessed using repeated applications of saturating ATP (300 μM). Application of BzATP together with light (300 s) resulted in a small but persistent current and a significant decrease in the maximal ATP response (43 ± 2%, n = 12, P < 0.0001) (Figure 3A). Both effects were absent in cells that were perfused with BzATP but were not exposed to light (Figure 3B). It is important to note that even after 300 s of illumination, the incorporation was still not complete, because a fraction of the receptors was still responding to ATP. The dose–response curves for ATP were

Table 1

EC_{50} values and Hill coefficients for various ligands on the P2X2 and P2X2/1 receptor chimera

Receptor	Ligand	EC_{50} (nM)	Hill coefficient	Relative efficacy	*n* (cells)
P2X2	ATP	36 000 ± 2000	1.5 ± 0.1	1	5
	BzATP	75 000 ± 2000	2.2 ± 0.1	~0.2	5
Chimera	ATP	3 ± 0.4	1.2 ± 0.2	1	7
	BzATP	27 ± 4	1.4 ± 0.2	~1	9
	αβ-MetATP	137 ± 6	1.6 ± 0.1	~1	21–34
	TNP-ATP	20 ± 3	0.9 ± 0.1	~0.02	4–7

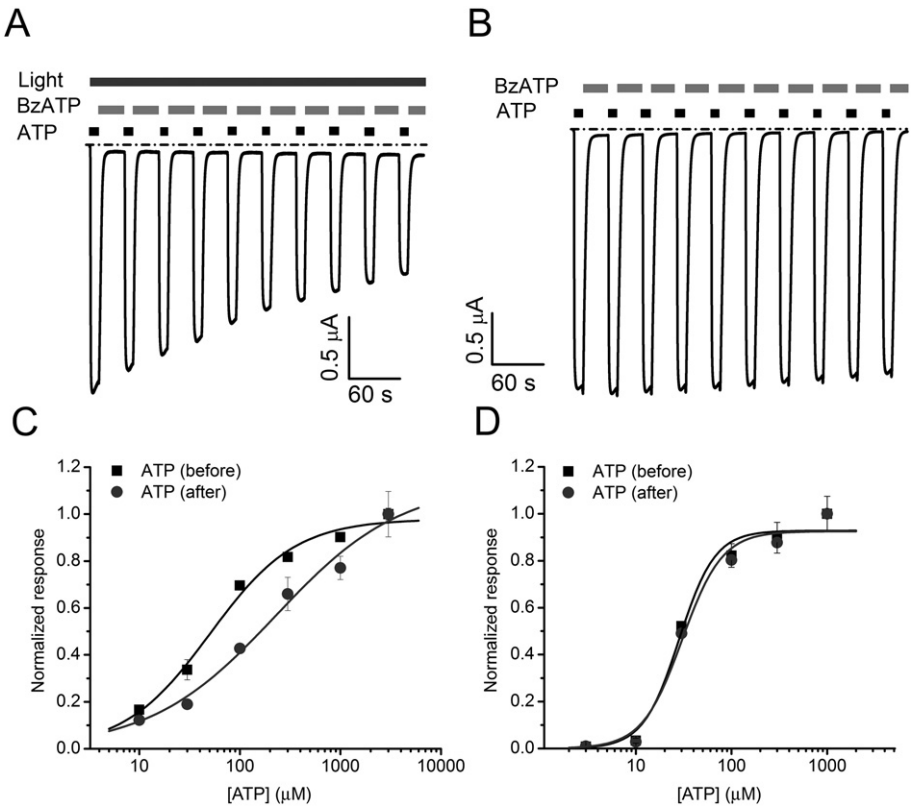

Figure 3

Photo-incorporation of BzATP in P2X2 receptors. Current traces are shown after repetitive application (300 s) of ATP (300 µM) and BzATP (30 µM) on a P2X2R-expressing oocyte (A) with and (B) without UV light. Dose–response curves of ATP for P2X2 receptors were measured before and after repetitive application of ATP (300 µM) and BzATP (30 µM) for both conditions: (C) in the presence of UV-light treatment (n = 5–11 cells) and (D) when no UV light was illuminated (n = 11 cells). Data are presented as mean ± SEM.

determined before and after (300 s) covalent incorporation of BzATP on the P2X2 receptors (Figure 3C). Interestingly, both the potency (56 ± 11 vs. 154 ± 55 µM, $P < 0.01$) and the cooperativity (1.1 ± 0.1 vs. 0.8 ± 0.1, n = 5–11, $P = 0.18$) of ATP decreased after covalent incorporation of BzATP (Figure 3C). On the other hand, potency (28.2 ± 4 vs. 30.3 ± 5 µM, $P > 0.05$) and cooperativity (2.3 ± 0.7 vs. 2.0 ± 0.6, n = 7, $P > 0.05$) of ATP remain unchanged for the BzATP treatment when UV light was not illuminated (Figure 3D). Taken together, these results suggest that photo-incorporation of a partial agonist (BzATP) into the ATP-binding sites in P2X2 receptors could modulate ATP response.

Time course of covalent activation of P2X2/1 receptor chimera

Unlike P2X1 receptors, the P2X2/1 receptor chimera does not desensitize, which facilitates studies with covalent agonists. Moreover, BzATP is a full agonist of the P2X2/1 receptor chimera (Figure 2). Therefore, we decided to further conduct our binding/gating study using the P2X2/1 receptor chimera.

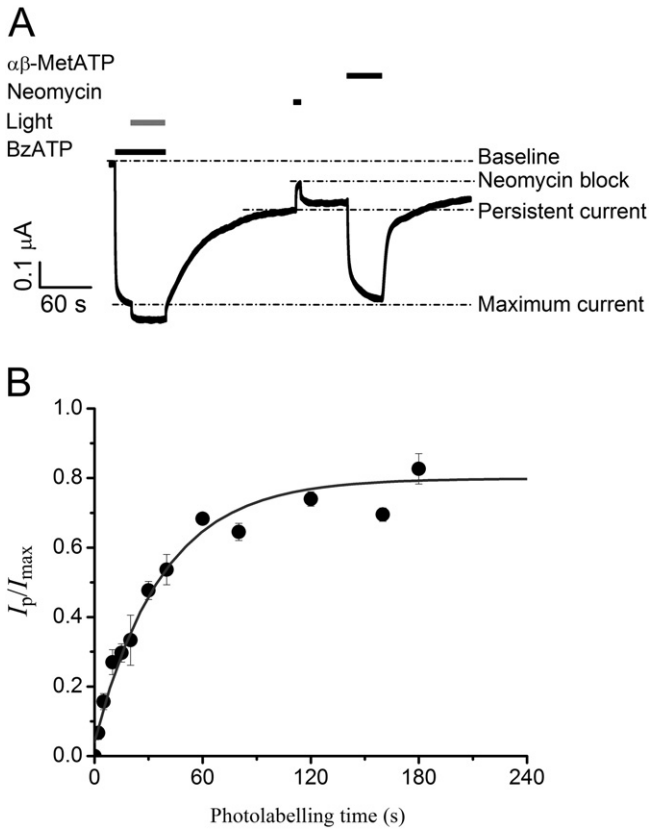

Figure 4

Time course of photo-incorporation of BzATP on the P2X2/1 receptor chimera. (A) Representative current trace showing persistent current after photolabelling of the P2X2/1 receptor chimera by 1 μM BzATP. UV-light application leads to photolabelling, as shown by persistent current specifically blocked by 3 mM neomycin. The block generated by neomycin was completely reversible. After photolabelling, the remaining closed receptors could be activated by the application of a full agonist, for example, 1 μM αβ-MetATP. A light-induced artefact is also visible in the trace, but it was completely reversible. (B) Time course of photolabelling of P2X2/1 receptor chimera by BzATP. Ratio between persistent current (I_p) and the total current (I_{max}) from the P2X2/1 receptor chimera after photolabelling was plotted against different time intervals for irradiation. Mono-exponential fit of the curve gave a time constant of (τ) = 37 ± 5 s. Data are presented as mean ± SEM of 3–11 cells for each time point.

We first determined the photo-incorporation time course of BzATP using a super-saturating concentration (1 μM). UV light was shone onto the oocyte only after the BzATP current had reached a steady state, that is, after occupying all the binding sites (Figure 4A). After photolabelling, oocytes were washed in the dark for at least three times the time normally required for complete deactivation of P2X2/1 receptor chimera receptors (measured in the absence of UV light), in order to ensure complete dissociation of non-covalently attached BzATP. During photolabelling, we observed photo-potentiation of the BzATP current, that is, a fast increase in inward currents above the maximum activation of the P2X2/1 receptor chimera at a saturating concentration of BzATP (Figure 4A). We do not know the origin of these light-induced artefacts, but because they were completely reversible, they did not affect our subsequent analysis and therefore were ignored in all our analyses. After photolabelling, we observed a persistent current (I_p) originating from P2X2/1 receptor chimeras locked in the open conformation, as evidenced by perfusion of neomycin (3 mM), a partial open channel blocker of the P2X2/1 receptor chimera (Bongartz *et al.*, 2010). The time course of the photolabelling was calculated by plotting the degree of persistent activation (I_p/I_{max}, where I_{max} is the maximal current evoked by 1 μM αβ-MetATP after photolabelling) as a function of irradiation time (Figure 4B). We used αβ-MetATP to assess the maximal current because this full agonist dissociates from the P2X2/1 receptor chimera much more rapidly (τ = 2.5 ± 0.3 s) than BzATP (τ = 23.8 ± 0.5 s) or ATP (τ = 63 ± 2 s) (Rettinger and Schmalzing, 2004). We found that perfusion and illumination for 2 s resulted in 2.0 ± 0.3% persistent activation, whereas a longer treatment (40 s) led to 54 ± 4% persistent activation (Table 2).

Enriching a population of channels

During the time course of photolabelling, binding site occupancy increases, making it possible to enrich a population of P2X2/1 receptor chimeras with one or two agonists bound. In order to calculate the fractional distribution $f(x)$ of unliganded, monoliganded, diliganded and triliganded receptors after different irradiation times, we used the following equation (Equation 1):

$$f(x) = \frac{n!(p^x q^{n-x})}{[(n-x)!x!]} \quad (1)$$

Table 2

EC_{50} values and Hill coefficient for αβ-MetATP on the P2X2/1 receptor chimera

Photolabelling time (s)	% Covalent activation	EC_{50} (nM)	Hill coefficient	*n* (cells)
0	0	137 ± 6	1.6 ± 0.1	21–34
2	2 ± 0.3	118 ± 8	1.2 ± 0.1	5–12
20	33 ± 7	87 ± 12	1.1 ± 0.1	5
40	54 ± 4	101 ± 18	0.9 ± 0.1	8–10

where n is the total number of ligand-binding sites per receptor, p is the probability that a particular site is labelled, q is the probability that a particular site is not labelled ($1–p$) and x is the number of covalently bound BzATP molecules. P2X receptors are trimeric receptors with three agonist-binding pockets (Kawate *et al.*, 2009), therefore $n = 3$. For calculating fraction occupancies, we made one assumption. We assumed that covalent labelling occurs randomly and with similar efficiency in all binding sites. This assumption is supported by the fact that photolabelling was performed at a super-saturating concentration of BzATP (1 μM; EC_{50} = 27 nM), ensuring that all binding sites are occupied at all times irrespective of the individual binding site affinities. In addition, benzophenones photogenerate reactive entities (radicals) that can insert into C–H bonds but do not react efficiently with water (Kapfer *et al.*, 1995). BzATP should therefore photo-incorporate into the ATP-binding sites with similar efficiency irrespective of the nature of the proximal amino acid, the presence of water molecules in the binding site or the conformational state of the receptor.

We then considered two models for kinetically describing the observed persistent current after photolabelling: model A, where binding of three agonist molecules is required to open the channel, and binding of less than three agonists is not sufficient for gating, and model B, where binding of two or more agonists is sufficient to open the channel with full efficacy respectively. Monoliganded channels were considered as closed in this model. We did not consider models where one agonist is sufficient to open the channel, as opening of P2X receptors is known to be highly cooperative (Ding and Sachs, 1999; Li *et al.*, 2008; Evans, 2009). It is important to mention here that we did not consider models where opening probabilities were lower than 1 for the BzATP-induced current because they generated complex equations with too many variables, which would lead to an over-interpretation of our results.

For model A, Equation 1 yields:

$$f(3) = p^3 \text{ or } p = f(3)^{1/3} = \left(\frac{I_p}{I_{max}}\right)^{1/3}$$

with (I_p/I_{max}) determined from electrophysiological recordings (Figure 4B). Thus, the probability that any site is labelled after 2 and 40 s irradiation is 27 and 81%, respectively. The statistical distribution of channels $f(x)$ containing 0, 1, 2 and 3 bound ligands is then predicted to be 0.39, 0.43 and 0.15 and 0.02 for 2 s of irradiation, and 0.006, 0.09 and 0.37 and 0.54 for 40 s of irradiation, respectively.

For model B, Equation 1 yields:

$$\frac{I_p}{I_{max}} = f(2) + f(3) = 3p^2 - 2p^3$$

Thus, the probability that any site is labelled after 2 and 40 s irradiation is 8 and 53%, respectively. The statistical distribution of channels $f(x)$ containing 0, 1, 2 and 3 bound ligands is then predicted to be 0.77, 0.21 and 0.02 and 0 for 2 s of irradiation, and 0.11, 0.35 and 0.39 and 0.15 for 40 s of irradiation, respectively.

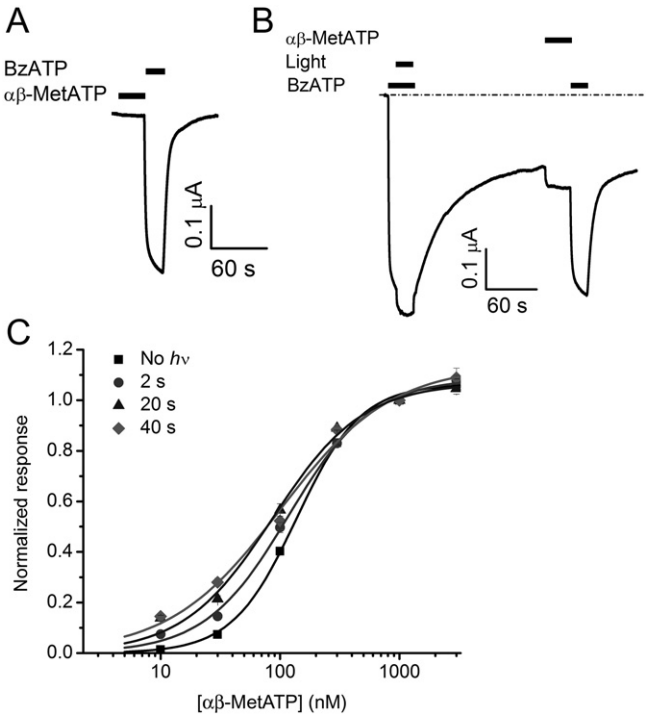

Figure 5

Occupancy with BzATP increases the efficacy and potency of αβ-MetATP. Representative current traces of 10 nM αβ-MetATP on the P2X2/1 receptor chimera (A) before and (B) after photolabelling for 20 s with 1 μM BzATP. (C) Dose–response curves for αβ-MetATP on the P2X2/1 receptor chimera were determined before and after 2, 20 and 40 s of photolabelling. The curves shifted leftward upon progressive photolabelling. Data are presented as mean ± SEM of 5–34 cells for each concentration of ligand.

Occupancy with a full agonist increases the efficacy and potency of partial agonists

We now tested the possibility whether pre-occupancy of receptors with a full agonist (BzATP) could modulate the response of perfused agonists. We photolabelled the P2X2/1 receptor chimeras with BzATP for 2, 20 or 40 s (irradiation times that lead to partial BzATP covalent incorporation) and subsequently determined a dose–response curve for the full agonist αβ-MetATP. Unlike P2X2 receptors, on the P2X2/1 receptor chimera pre-occupancy with BzATP increased the potency for αβ-MetATP (leftward shift in the dose–response curves) and lowered the Hill number without affecting the maximum current (Figure 5A–C and Table 2), which is expected as fewer and fewer ligands are needed to fully occupy and open the channel as the time of photolabelling will increase.

We then wondered how partial occupancy with BzATP could modulate the response to TNP-ATP, a partial agonist with low efficacy for the P2X2/1 receptor chimera (<2% current at saturating TNP-ATP concentration). We photolabelled the P2X2/1 receptor chimera for 2 or 40 s, and performed a subsequent dose–response curves for TNP-ATP. We found that the relative efficacy of TNP-ATP increased from 2 (no *hν*) to 6% (after 2 s) and 12% (after 40 s photolabelling; Figure 6A–C and Table 3). Hill numbers also decreased with

Table 3

EC_{50} values and Hill coefficients for TNP-ATP on the P2X2/1 receptor chimera

Time of photolabelling (s)	% Covalent activation	EC_{50} value (nM)	Hill coefficient	*n* (cells)
0	0	13 ± 3	1.1 ± 0.2	4–7
2	2 ± 0.3	16 ± 2	0.8 ± 0.1	3–8
40	54 ± 4	13 ± 4	0.6 ± 0.1	5–11

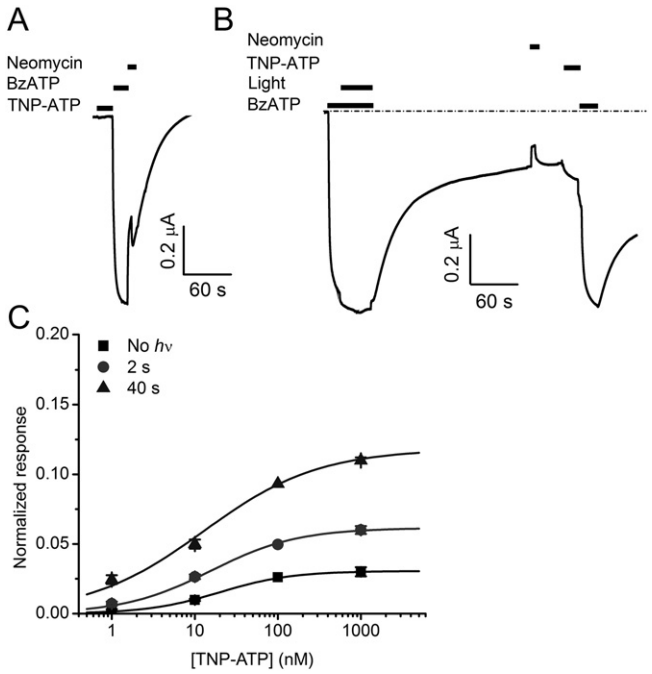

Figure 6

Occupancy with BzATP increases the efficacy and potency of TNP-ATP. Representative current traces of 1 µM BzATP and 300 nM TNP-ATP on the P2X2/1 receptor chimera (A) before and (B) after photolabelling for 40 s. (C) Dose–response curves for TNP-ATP on the P2X2/1 receptor chimera were determined before and after 2 and 40 s of UV-light irradiation. The curves showed an increase in the maximal response by TNP-ATP on the P2X2/1 receptor chimera upon progressive photolabelling. All dose–response curves were normalized to the response generated by 1 µM BzATP before photolabelling. Data are presented as mean ± SEM of 3–11 cells for each ligand concentration.

irradiation time, while EC_{50} seemed unaffected. We then tested which model (model A or B) best fitted our data obtained with TNP-ATP.

For model A, TNP-ATP-induced current can arise from receptors that are non-liganded, monoliganded or diliganded, leading to the following equation:

$$\frac{I_{\mathrm{TNP}}}{I_{\mathrm{BzATP}}} = Af(0) + Bf(1) + Cf(2) \qquad (2)$$

where A is the opening probability of receptors containing three TNP-ATP, B is the opening probability of receptors containing two TNP-ATP and one covalently bound BzATP, and C is the opening probability of receptors containing one TNP-ATP and two covalently bound BzATP. We know that $A = 2\%$ (Figure 2F). After 2 and 40 s irradiation, Equation 2 yields:

$$\text{At } t = 2 \text{ s}, I_{TNP}/I_{\mathrm{BzATP}} = 0.06 = 0.02 \times 0.39 + 0.43B + 0.16C$$

$$\text{At t} = 40 \text{ s}, \mathrm{I_{TNP}}/\mathrm{I_{BzATP}} = 0.12 = 0.02 \times 0.007 + 0.09B + 0.37C$$

This gives $B = 0.2\%$ and $C = 32\%$.

The value for B (0.2%) is unexpectedly lower than that of A (2%), but we believe this value to be within the range of error of our measurements. Therefore, our calculation implies that receptors with three TNP-ATP or two TNP-ATP and one covalently attached BzATP have a very low opening probability; only receptors with one TNP-ATP and two covalently attached BzATP would open substantially (32%) after application of a saturating concentration of TNP-ATP.

For model B, TNP-induced current can arise from receptors that are either non-liganded (0 covalently attached BzATP) or monoliganded (with one covalently attached BzATP), leading to the following equation:

$$\frac{I_{\mathrm{TNP}}}{I_{\mathrm{BzATP}}} = Af(0) + Bf(1) \qquad (3)$$

where A is the opening probability of receptors containing three TNP-ATP and B is the opening probability of receptors containing two TNP-ATP and one covalently bound BzATP. We know that $A = 2\%$ (Figure 2F). After 2 and 40 s irradiation, Equation 3 yields:

$$\text{At } t = 2 \text{ s}, I_{\mathrm{TNP}}/I_{\mathrm{BzATP}} = 0.06 = 0.02 \times 0.77 + 0.21B$$

$$\text{At t} = 40 \text{ s}, \mathrm{I_{TNP}}/\mathrm{I_{BzATP}} = 0.12 = 0.02 \times 0.11 + 0.35B$$

This gives us two different values for B, 0.21 and 0.33, making this model less likely.

Discussion

In the current study, we have used photolabelling-coupled electrophysiology to trap P2X receptors in various liganded states and study the relationship between binding site occupancy and channel gating. Photolabelling has been coupled to electrophysiology to study allosteric mechanisms in ligand-gated ion channels using both whole cell (Mourot *et al.*, 2006; Zhong *et al.*, 2008; Agboh *et al.*, 2009) and excised patches (Brown *et al.*, 1993; Ruiz and Karpen, 1997;

Forman *et al.*, 2007). Here, we used a custom-made oocyte recording chamber that allowed successful photolabelling and measure of current from the same population of receptors in real time without the need for excising patches. Incorporation of BzATP was robust, both on P2X2 and on P2X2/1 receptor chimera, and increased with illumination time, most probably through a mechanism of photoaffinity labelling.

After cross-linking a partial agonist (BzATP) onto P2X2 receptors, the saturating ATP response was diminished, which is in agreement with BzATP occupying a fraction of the agonist binding sites, thereby preventing full occupancy and full activation with ATP. The EC_{50} for ATP also decreased for the receptors covalently labelled with BzATP as compared with the unlabelled P2X2 receptors (Figure 3C,D). This can be explained by the fact that BzATP, even though being a partial agonist of P2X2 receptors, acts like a competitive, insurmountable antagonist of ATP, producing a rightward shift of the ATP dose–response curve together with a depression of the maximal response.

Using the P2X2/1 receptor chimera, which does not desensitize, we observed an increase in the potency of agonists (leftward shift in the dose–response curves) together with a decrease in cooperativity (lower Hill number) upon progressive photolabelling with the full agonist BzATP (Figure 5C). This is in agreement with the binding steps not being independent but strongly and positively cooperative (Ding and Sachs, 1999). Strong interactions between subunits for channel activation were also reported for P2X2 receptors and cyclic nucleotide-gated (CNG) ion channels (Karpen and Brown, 1996; Jiang *et al.*, 2011).

TNP-ATP, which is a partial agonist with very low efficacy, becomes more effective only after progressive BzATP photolabelling (Figure 6C). The increase in efficacy is expected from a channel that is partially liganded with a full agonist, as the probability that the channel is fully liganded is higher at any TNP-ATP concentration. Unlike the agonist αβ-MetATP, we did not observe a significant increase in potency for TNP-ATP during progressive photolabelling (Figure 6C). Although unexpected, this result could be due to the difficulty in resolving very small currents induced by sub-saturating concentrations of the TNP-ATP (partial agonist with very low efficiency).

The use of covalently bound ligands enables experiments that are not possible or difficult to perform with freely diffusing ones. After covalent attachment, it is, for example, possible to add another ligand at saturating concentrations to occupy the remaining binding sites, without the complication of the two ligands competing. In such an experiment, we applied TNP-ATP (partial agonist with very low efficacy) onto receptors partially liganded with a full agonist (after 2 or 40 s irradiation with BzATP). We found that application of TNP-ATP always induced potentiation (but never reduction) of the current (Figure 5C). Partial agonists are sometimes thought of as ligands that display both agonistic and antagonistic effects. Our data seem to show that partial agonists are nothing but agonists, although of much lower efficacy than full agonists.

Another advantage of covalently bound ligands is that the relationship between binding site occupancy and channel gating can be studied, without the complication arising from binding/unbinding events. In a landmark study, Ruiz and Karpen (1997) managed to observe single CNG channels with exactly one, two, three or four cGMP agonist molecules bound, and to extract the opening probabilities for each liganded state. As our recordings were performed on a population of ion channels, it was not possible to extract opening probabilities of each liganded state. We have used two simple models to fit our data: model A, where binding of three agonists is required to open the channel, and model B, where binding of two or more agonists is sufficient to open the channel. The model (model A) where only three bound agonists are able to open the channel could nicely describe the observed increase in efficacy of TNP-ATP after progressive labelling. In contrast, the second model (model B), where binding of two agonist molecules already leads to maximum opening, appeared to be less successful in describing our experimental observations. More complex models were not taken into account because we believe that this would have led to an over-interpretation of our experimental findings. Therefore, we are aware that a more complete understanding of the relationship between binding and gating will require extending this strategy to analogous experiments at the single-channel level.

Acknowledgements

Y B was supported by a fellowship from International Max Planck Research School. We are thankful to Prof. Ernst Bamberg for his support.

Conflicts of interest

None.

References

Agboh KC, Powell AJ, Evans RJ (2009). Characterisation of ATP analogues to cross-link and label P2X receptors. Neuropharmacology 56: 230–236.

Aschrafi A, Sadtler S, Niculescu C, Rettinger J, Schmalzing G (2004). Trimeric architecture of homomeric P2X2 and heteromeric P2X1+2 receptor subtypes. J Mol Biol 342: 333–343.

Barrera NP, Ormond SJ, Henderson RM, Murrell-Lagnado RD, Edwardson JM (2005). Atomic force microscopy imaging demonstrates that P2X2 receptors are trimers but that P2X6 receptor subunits do not oligomerize. J Biol Chem 280: 10759–10765.

Biskup C, Kusch J, Schulz E, Nache V, Schwede F, Lehmann F *et al.* (2007). Relating ligand binding to activation gating in CNGA2 channels. Nature 446: 440–443.

Bongartz EV, Rettinger J, Hausmann R (2010). Aminoglycoside block of P2X2 receptors heterologously expressed in Xenopus laevis oocytes. Purinergic Signal 6: 393–403.

Brown RL, Gerber WV, Karpen JW (1993). Specific labeling and permanent activation of the retinal rod cGMP-activated channel by the photoaffinity analog 8-p-azidophenacylthio-cGMP. Proc Natl Acad Sci U S A 90: 5369–5373.

Ding S, Sachs F (1999). Single channel properties of P2X2 purinoceptors. J Gen Physiol 113: 695–720.

Erb L, Lustig KD, Ahmed AH, Gonzalez FA, Weisman GA (1990). Covalent incorporation of 3′-O-(4-benzoyl)benzoyl-ATP into a P2 purinoceptor in transformed mouse fibroblasts. J Biol Chem 265: 7424–7431.

Evans RJ (2009). Orthosteric and allosteric binding sites of P2X receptors. Eur Biophys J 38: 319–327.

Forman SA, Zhou QL, Stewart DS (2007). Photoactivated 3-azioctanol irreversibly desensitizes muscle nicotinic ACh receptors via interactions at alphaE262. Biochemistry 46: 11911–11918.

Jiang R, Lemoine D, Martz A, Taly A, Gonin S, Prado de Carvalho L *et al*. (2011). Agonist trapped in ATP-binding sites of the P2X2 receptor. Proc Natl Acad Sci U S A 108: 9066–9071.

Kapfer I, Jacques P, Toubal H, Goeldner MP (1995). Comparative photoaffinity labeling study between azidophenyl, difluoroazidophenyl, and tetrafluoroazidophenyl derivatives for the GABA-gated chloride channels. Bioconjug Chem 6: 109–114.

Karpen JW, Brown RL (1996). Covalent activation of retinal rod cGMP-gated channels reveals a functional heterogeneity in the ligand binding sites. J Gen Physiol 107: 169–181.

Karpen JW, Ruiz M (2002). Ion channels: does each subunit do something on its own? Trends Biochem Sci 27: 402–409.

Kawate T, Michel JC, Birdsong WT, Gouaux E (2009). Crystal structure of the ATP-gated P2X4 ion channel in the closed state. Nature 460: 592–598.

Khakh BS, North RA (2006). P2X receptors as cell-surface ATP sensors in health and disease. Nature 442: 527–532.

Kilkenny C, Browne W, Cuthill IC, Emerson M, Altman DG (2010). NC3Rs Reporting Guidelines Working Group. Br J Pharmacol 160: 1577–1579.

Le Novere N, Changeux JP (1999). The Ligand Gated Ion Channel Database. Nucleic Acids Res 27: 340–342.

Li M, Chang TH, Silberberg SD, Swartz KJ (2008). Gating the pore of P2X receptor channels. Nat Neurosci 11: 883–887.

McGrath J, Drummond G, McLachlan E, Kilkenny C, Wainwright C (2010). Guidelines for reporting experiments involving animals: the ARRIVE guidelines. Br J Pharmacol 160: 1573–1576.

Marquez-Klaka B, Rettinger J, Bhargava Y, Eisele T, Nicke A (2007). Identification of an intersubunit cross-link between substituted cysteine residues located in the putative ATP binding site of the P2X1 receptor. J Neurosci 27: 1456–1466.

Mourot A, Kotzyba-Hibert F, Goeldner M, Bamberg E (2006). Photo-induced covalent attachment of agonists as a tool to study allosteric mechanisms of nicotinic acetylcholine receptors. J Mol Neurosci 30: 3–4.

Mourot A, Bamberg E, Rettinger J (2008). Agonist- and competitive antagonist-induced movement of loop 5 on the alpha subunit of the neuronal alpha4beta4 nicotinic acetylcholine receptor. J Neurochem 105: 413–424.

Nicke A, Baumert HG, Rettinger J, Eichele A, Lambrecht G, Mutschler E *et al*. (1998). P2X1 and P2X3 receptors form stable trimers: a novel structural motif of ligand-gated ion channels. EMBO J 17: 3016–3028.

North RA (2002). Molecular physiology of P2X receptors. Physiol Rev 82: 1013–1067.

North RA, Surprenant A (2000). Pharmacology of cloned P2X receptors. Annu Rev Pharmacol Toxicol 40: 563–580.

Rettinger J, Schmalzing G (2003). Activation and desensitization of the recombinant P2X1 receptor at nanomolar ATP concentrations. J Gen Physiol 121: 451–461.

Rettinger J, Schmalzing G (2004). Desensitization masks nanomolar potency of ATP for the P2X1 receptor. J Biol Chem 279: 6426–6433.

Ruiz ML, Karpen JW (1997). Single cyclic nucleotide-gated channels locked in different ligand-bound states. Nature 389: 389–392.

Valera S, Hussy N, Evans RJ, Adami N, North RA, Surprenant A *et al*. (1994). A new class of ligand-gated ion channel defined by P2x receptor for extracellular ATP. Nature 371: 516–519.

Virginio C, Robertson G, Surprenant A, North RA (1998). Trinitrophenyl-substituted nucleotides are potent antagonists selective for P2X1, P2X3, and heteromeric P2X2/3 receptors. Mol Pharmacol 53: 969–973.

Werner P, Seward EP, Buell GN, North RA (1996). Domains of P2X receptors involved in desensitization. Proc Natl Acad Sci U S A 93: 15485–15490.

Zhong H, Rusch D, Forman SA (2008). Photo-activated azi-etomidate, a general anesthetic photolabel, irreversibly enhances gating and desensitization of gamma-aminobutyric acid type A receptors. Anesthesiology 108: 103–112.